Genetic Analysis of *Arabidopsis* Metacaspases as Regulators of Responses to DNA Damage in Root Stem Cells

By

CHIA-HUI CHEN

A thesis submitted to the

Graduate School-New Brunswick

Rutgers, The State University of New Jersey

In partial fulfillment of the requirements

For the degree of

Master of Science

Graduate Program in Plant Biology

Written under the direction of

Dr. Eric Lam

And approved by

_____

_____

_____

New Brunswick, New Jersey

October 2016

ABSTRACT OF THE THESIS

Genetic Analysis of *Arabidopsis* Metacaspases as Regulators of Responses to DNA Damage in Root Stem Cells

By Chia-Hui Chen

Thesis Director:
Dr. Eric Lam

Metacaspases (MCPs), are highly conserved caspase-related cysteine proteases that may play important roles in controlling programmed cell death (PCD) in plants. *Arabidopsis thaliana* has nine metacaspases, and they could be divided into Type Ⅰ (AtMC1-3) and Type Ⅱ (AtMC4-9), based on their predicted protein sequences. Recent research indicates the function for some of the AtMCs; however, there are many difficulties in studying plant PCD: Single gene mutations produce only quantitative effects and are often quite variable, suggesting that potential functional redundancy among members of this multigene family and parallel pathways may confound interpretation of phenotypes.

In this thesis work, I explored a well-defined DNA damage response (DDR) of root

stem cells as an excellent cellular model for PCD studies in plants. Root stem cells have been shown to exhibit low resistance to genotoxic stresses. To maintain the integrity of the genome, plant root stem cells induce different downstream consequences such as DNA repair mechanisms, cell-cycle arrest, or PCD upon excess DNA damage that is correlated with elongation arrest of the root.

Compared with wild-type plants, the root tip of *atmc2*, *atmc4*, *atmc2/4*, *atmc9* and *atmc4/9* gene knockout mutants show a lower suppression effect of primary root elongation after zeocin treatment, a genotoxic radiomimetic drug that initially causes cell death in the root stem cell niche and inducing DNA double-strand breaks (DSBs). Among these 3 *AtMC* genes studied, my results showed that *atmc9* mutant displayed the highest resistance to zeocin treatment and but no significant difference between the *atmc4/9* double mutant and the single gene mutants in terms of root elongation. Interestingly, the *atmc4/9* double mutant showed a dramatic suppression of PCD at the root stem cell niche compared to the other genotypes examined. Taken together, these results indicate that *AtMC2*, *AtMC4*, and *AtMC9* might work as positive regulators in the Zeocin-activated PCD process in the *Arabidopsis* root stem cell niche and *AtMC9* plays the most important role than other two genes.

ACKNOWLEDGEMENTS

It is a pleasure to thank the people who made this thesis possible. I would never have been able to finish it without the guidance of my advisor and assistance of my committee members. This work was supported by a National Science Foundation grant (IOS-1258071).

TABLE OF CONTENTS

LIST OF TABLES

LIST OF FIGUERS

1. Introduction

1.1 Introduction of Programmed Cell Death

Programmed cell death (PCD) is a genetically controlled process that helps to eliminate unwanted or damaged cells during development or biological stresses. It happens not only in animals, but in fungi and plants too (Lam, 2004; He et al., 2008). Plant PCD can be initiated by many factors, for example: PCD is linked to vacuole collapse, which is necessary for the differentiation of a tracheary element (TE) in the xylem (Lam, 2004; Benneau et al., 2008). In addition, external environmental factors, such as pathogen challenges, trigger a rapid cell death process during a hypersensitive response in the plant immune system (Lam, 2004; Coll et al., 2011).

1.2 Enzyme Participation in PCD

Caspases, which have specific cysteine protease activity, play a crucial role in PCD in metazoan animals (Cohen, 1997; Andersen et al., 2005). Initiator caspases (caspase 2, caspase 8, and caspase 9) are involved in apoptosis signaling cascades and they are necessary for the activation of executioner caspases (caspase 3, caspase 6, and caspase 7). The executioner caspases cleave numerous substrates that lead to different phenotypic

changes during apoptosis (Vercammen et al., 2007; Tait and Green, 2010).

1.3 Introduction of Metacaspase (MCs)

Based on the structural homologies with the caspases, a group of caspase- like proteases have been identified in plant, fungi, and protozoa that are designated as metacaspases (MCs) (Uren et al., 2000; Vercammen et al., 2007; Tsiatsiani et al. 2011; Lam and Zhang, 2012; Fagundes et al., 2015), and have 20kDa (p20) and 10kDa (p10) subunits. The activation of caspases and some MCs can also be accomplished by an autolytic process that requires the active-site cysteine residue of these enzymes (Vercammen et al., 2004; Watanabe and Lam, 2011). Despite having a similar secondary structure, caspase and MC families do not share a high degree of sequence similarities (Cambra et al., 2010). The preferred cleavage site amino acid for caspases and MCs is different too. Unlike caspases, the critical P1 residue at specific substrate sites for MCs are either arginine or lysine, while aspartate is the preferred residue for caspase target sites **(**Vercammen et al. 2004; Bozhkov et al., 2005; Watanabe and Lam, 2005**)**. Due to these differences, MCs cannot be categorized as caspases.

1.4 Metacaspases in *Arabidopsis thaliana* (AtMCs)

Arabidopsis thaliana has nine MCs (Vercammen *et al*., 2004; Watanabe and Lam,

2004). Based on their domain structure and sequence similarities, these proteases can be divided into either Type I (AtMC1-*3*) or Type II (AtMC4-*9*) MCs (Uren *et al.*, 2000; Bonneau *et al.*, 2008; Tsiatsiani *et al*., 2011; Watanabe and Lam, 2011). There are many differences between Type I and Type II MCs:

1. Type I MCs are found in plant, algae, protozoa and fungi, in addition to some bacteria phylla; Type II MCs can only be detected in higher plants and some photosynthetic eukaryotes such as volvox (Tsiatsiani et al. 2011; Lam and Zhang, 2012).
2. The 3 Type I MC-encoding genes are dispersed between chromosome 1, chromosome 4, and chromosome 5 of *Arabidopsis*, however most of the Type II MC-encoding genes are clustered on Chr. 1, except for AtMC9 being located on Chr. 5. The phylogenetic relationship and diversity of AtMCs are both shown below:

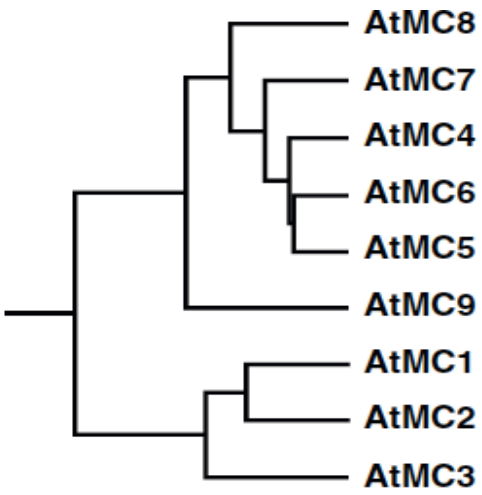

Figure 1 Phylogenetic tree of nine *Arabidopsis* MCs. (modified from Lam and Zhang, 2012).

3. Type I MCs have shorter linker regions between the p20- and p10- like domains when compared with Type II MCs (Watanabe and Lam, 2011; Lam and Zhang, 2012). The linker region of Type II MCs is variable in size and sequence, and it might be the key region that affects the different functions of Type II MCs. Unlike Type II MC activation, which requires autolytic cleavage, Type I MCs do not (Lam and Zhang, 2012).
4. Type I MCs contain an N-terminal pro-domain upstream of the p-20 domain, while Type II MCPs lack the apparent pro-domain (Coll *et al*., 2010; Lam and Zhang, 2012). The differences suggest that type I and type II MCs could be involved in different pathways in the programmed cell death process.

The structural differences between the two types of MCPs are shown in Fig. 2.

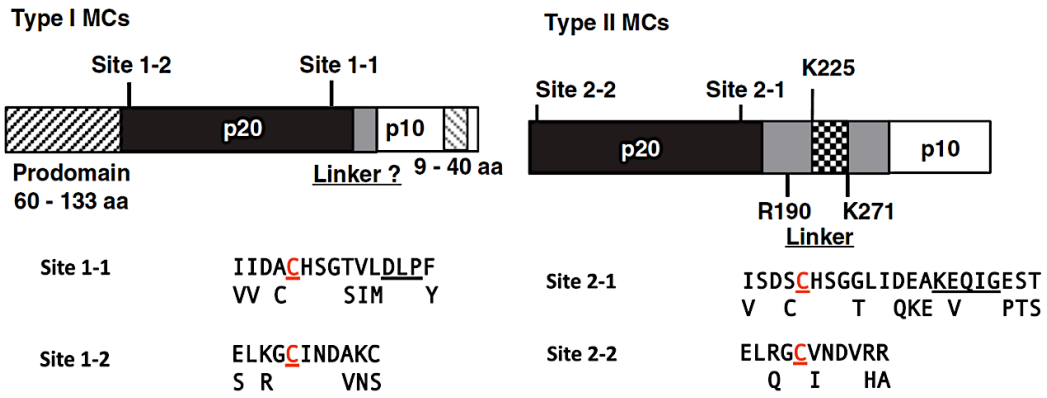

Figure 2 The domain structures of Type Ⅰ and Type Ⅱ MCs (modified from Lam and Zhang, 2012).

1.5 AtMCs Expression and Subcellular Location

The transcript expression levels for AtMCs vary in different tissues and at specific developmental stages (Zimmermann *et al*., 2004; Lam and Zhang, 2012; Kwon and Hwang, 2013). For Type I MCs in *Arabidopsis*, *AtMC1* and *AtMC3* have higher expression levels in most of the tissue types compared to that of *AtMC2*. Among Type II MCs, *AtMC4* is abundantly expressed in all tissues, while *AtMC9* is predominantly expressed in floral tissue.

Several studies found that different AtMCs have distinct optimal pH levels (Woltering, 2004). Vercammen *et al.* (2004) first reported that AtMC4 requires more basic pH (between pH 6.5-9.0) while AtMC9 prefers a lower pH (between pH 4.5-6.0) for their optimal activity. Furthermore, the optimal pH value for the activation of AtMC8 is reported to be between pH 7.5-8.5 (He *et al.,* 2008). According to previous results, different activation conditions for AtMCs depend on the pH environment, and it may lead to the localization diversity of AtMCs. For example, the Type I AtMC1 was reported to localize to the chloroplasts using a 35S::AtMC1::GFP fusion construct (Castillo-Olamenndi et al., 2007) while the green fluorescence of AtMC3:: GFP fusion protein can be observed in the nucleus (Kwon and Hwang, 2013). For Type II MCs, a AtMCP2d:: GFP fused protein can be detected strongly in the cytoplasm, but only weakly in the nucleus (Watanabe and Lam, 2011). Using 35S::AtMC9 lines, Vercammen et al. (2006) reported that overexpressed AtMC9 protein is localized to the apoplast. Another study generated the ProMC9::MC9 GFP reporter line, and indicated that AtMC9 also localizes in the nucleus and cytoplasm in *Arabidopsis* roots (Tsiatsiani et al. 2013).

1.6 Functional Analysis of AtMCs in PCD

Madeo et al. published the first report analyzing how MCs may function in

eukaryotes. The sole *Saccharomyces cerevisiae* MC (YCA1) is required for apoptosis-like cell death in yeast PCD under hydrogen peroxidase-induced oxidative stress (Madeo et al, 2002). Watanabe and Lam (2005) later demonstrated that AtMCP1b and AtMCP2b (aka AtMC1 and AtMC5, respectively) can partially complement a *yca1* deletion mutant to mediate oxidative stress-induced cell death in yeast.

Many studies presenting the functional analysis of MCs have been published during the past decade. After UV-irradiation, reactive oxygen species (ROS) or methyl viologen (MV) treatments, the expression of *AtMC8* increased rapidly in *Arabidopsis* seedlings. Transgenic over-expression of *AtMC8* in mutant plants increased ion leakage and protoplast cell death upon treatment with H_2O_2 or MV. In addition, two *AtMC8* knockout (KO) mutants were found to reduce sensitivity to MV. Based on these results, it has been suggested that AtMC8 is a positive regulator of plant PCD during oxidative stresses.

PCD can be induced as a reaction to plant pathogen attacks that lead to the hypersensitive responses (HR). This is an important component in the plant disease resistance response (Bozhkov and Lam, 2011). Recent studies indicate MCs are involved in this pathogen-induced PCD process. For Type I AtMCs in plants, it has been demonstrated that AtMC1 and AtMC2 regulate cell death due to biotic stress. AtMC1 is able to bind to LSD1, a negative regulator of HR-induced cell death, and AtMC2

apparently does not interact strongly with either AtMC1 or LSD1. AtMC1 is a positive regulator of BTH-induced PCD, and loss of AtMC2 resulted in more rapid BTH-induced cell death, suggesting that it is a negative regulator of PCD under these conditions. These Type I AtMCs appear to also play similar roles in the RPM1-mediated hypersensitive responses (HR) (Coll *et al.*, 2010). Furthermore, AtMC1 and autophagy may work positively in parallel pathways to regulate pathogen-triggered PCD (Coll et al., 2014).

As an abundantly expressed member amongst the 9 AtMCs, AtMC4 is a positive regulator in both biotic and abiotic stress (Watanabe and Lam, 2011). Compared to control plants, the over-expressed *AtMC4* transgenic plants resulted in stronger cell death responses; in contrast, the loss of *AtMC4* expression delayed cell death induced by either fumonisn B1 (FB1, a fungal toxin), acifluorfen (AF, an inhibitor of protoporphyrinogen oxidase and results in oxidative stress), or a *Pseudomonas syringae* pv. *maculicola* challenge.

TE cells are the elongated cells in xylem and are specialized for water transportation. PCD is required for TE differentiation (Tuner et al., 2007; Bollhöner et al., 2013). Recent studies found that the expression of *AtMC9* is involved in TE PCD as well as TE cell differentiation (Tuner et al., 2007; Ohashi-Ito et al., 2010). Compared to Col-0 WT plants, the *AtMC9* T-DNA insertion mutant delayed the vacuolar rupture process, and this

indicated that *AtMC9* is required for an efficient post mortem autolysis process (Bollhöner et al., 2013). Pepper (*Capsicum annuum* L.) metacaspase 9 (Camc9), is a Type II metacaspase which is homologous to AtMC9, and it is reported to act also as a positive regulator of pathogen-triggered PCD (Kim et al., 2013).

1.7 Introduction of DNA Damage Response

Genomic DNA is exposed to endogenous and external stresses every day that trigger DNA damage responses (DDR)(Garcia et al., 2003; Adachi et al., 2011). Living organisms induce different downstream processes such as DNA repair mechanisms, cell-cycle arrest, or apoptosis to preserve the integrity of their genome (Cicca and Elledge, 2010; Yoshiyama et al., 2014). ATAXIA-TELANGIECTASIA MUTATED (ATM) and ATM/RAD3-RELATED (ATR) are the key regulators in response to DNA damage (Yoshiyama et al., 2013). Consequently, the downstream regulatory pathways for these two signaling kinases can overlap (Shiloh, 2006; Cimprich and Cortez. 2008; Fulcher and Sablowski, 2009). The tumor suppressor p53 is a key transcription factor in animals, and plays a crucial role in the final determination of cell fate (Helton and Chen, 2007). Most DDR proteins are highly conserved in animals, plants, and fungi (Furukawa et al., 2010), although p53 protein cannot be found in plant genomes. However, the plant-specific

transcription factor Suppressor of Gamma Response 1(SOG1) has been suggested to be the functional orthologue of p53 (Yoshiyama et al., 2009; Yoshiyama et al., 2013). The DNA damage response pathway in plants is presented below.

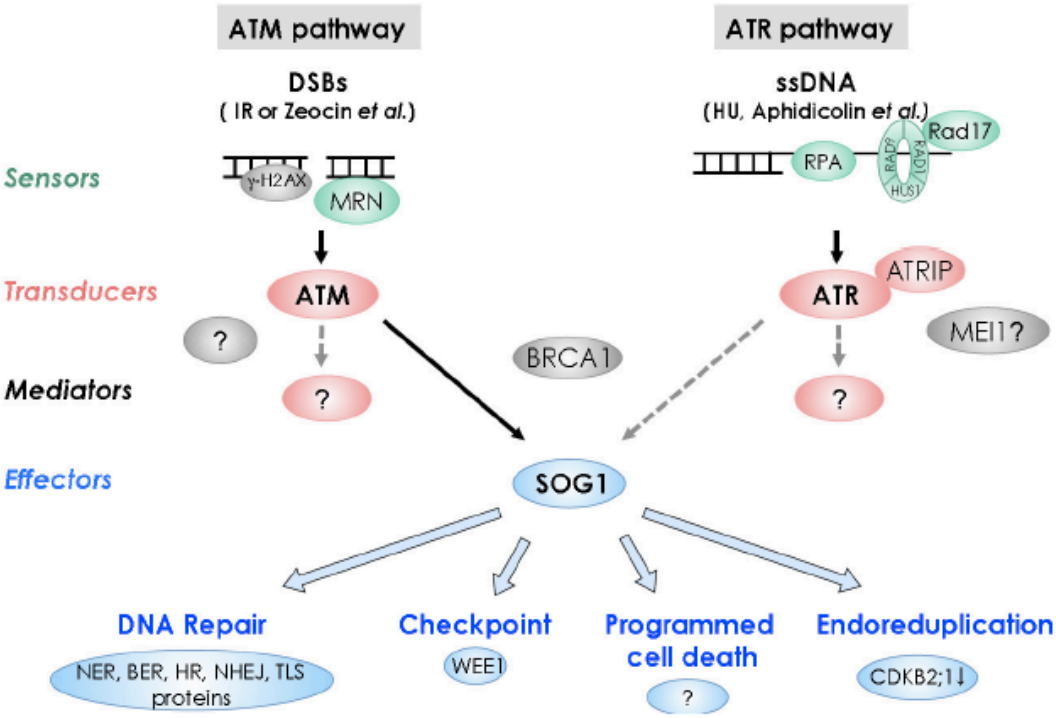

Figure 3 DNA damage response pathway in plants (Yoshiyama et al., 2013).

1.8 DDR Induced PCD Process in Plant Stem Cell Niche

In mammals, stem cells are known to be more sensitive to DNA damage than somatic cells, which activate downstream p53-dependent apoptosis to protect genome-stability and prevent cancer occurrences (Rich et al, 2000; Fulcher and

Sablowski, 2009; Yoshiyama et al., 2013). Recent studies showed that the DNA double strand break (DSB) inducers, such as Zeocin (a genotoxic, radiomimetic drug isolated from *Streptomyces*) or ionizing radiation (IR), can trigger PCD in *Arabidopsis* root and shoot stem cells. In addition, this DSB-induced PCD process was found to involve ATM, ATR, and SOG1 in *Arabidopsis*, thus beginning to define a genetic framework for DSB-induced PCD in plants (Fulcher and Sablowski, 2009; Furukawa et al., 2010). DSB-triggered PCD can also induce DNA endoreduplication and cell enlargement in *Arabidopsis* stem cells without changing of chromosome number (Adachi et al., 2011).

1.9 Objective

It has been over a decade since MCs were first identified in plants, and there is now viable evidence that MCs play an important role in plant programmed cell death progression. However, there are some difficulties when studying plant MCs: First, different MCs might have gene redundancy, so single MC gene mutants produce only small quantitative effects. Second, due to the potentially high level of redundancy with other parallel PCD pathways, the phenotypes of MC mutants might be difficult to ascertain with single gene mutants. Therefore, finding a suitable PCD model system is essential for accelerating MC research. This study explores the use of the DNA damage

response of *Arabidopsis* root stem cells as a new PCD model system to dissect the genetic function of *AtMC2* (a possible negative regulator), *AtMC4* (an abundantly expressed member of the Type II MC family found in all tissues), and *AtMC9* (a highly conserved Type II MC in plants that has a distinct structure and functional characteristics from other AtMCs) under DNA damage induced-stress.

2. Materials and Methods

2.1 Plant Material and Growth Conditions

All *Arabidopsis* metacaspase (AtMC) mutants and wild type control plants used in this study are in the *Arabidopsis thaliana* ecotype 'Columbia' (Col-0) genetic background. The *AtMC* mutant seeds of *atmc2-1* (SALK_002986), *atmc4-1* (SAIL_856_D05), and *atm 9* (SALK_075814) were obtained from the Salk Institute for Biological Studies (SALK) and Syngenta *Arabidopsis* Insertion Library (SAIL). The T-DNA insertion sites of each mutant line are presented in Fig. 3. The mutants and wild type seeds were sterilized in 3% sodium hypochlorite solution, sown onto germination media which contained 0.5X Murashige and Skoog salts with Gamborg vitamins (PhytoTechnology Laboratories), 1% sucrose (Fisher Chemical), 0.25% phytagel (Sigma), pH 5.7, and then were incubated at 4°C in the dark for 48h. After stratification, the plates were placed vertically at 21°C under long day conditions (16h light and 8h dark). Unless stated otherwise, the seedlings were transferred to soil after 7-10 days of growth on the germination plates.

***atmc2-1* (SALK_002986)**

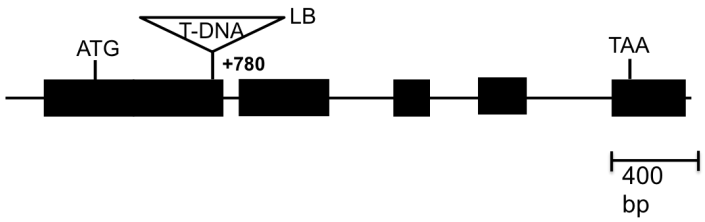

***atmc4-1* (SAIL_856_D05)**

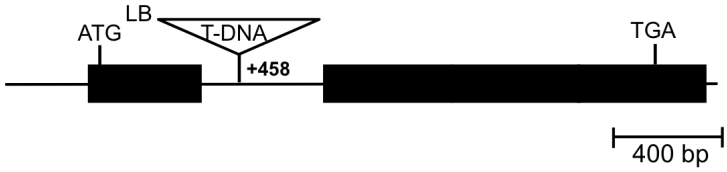

***atmc9* (SALK_075814)**

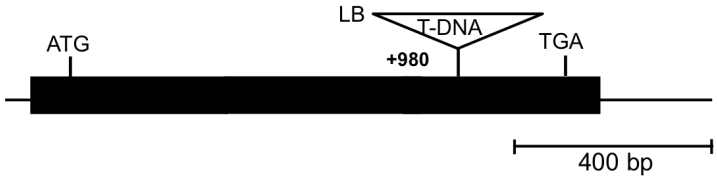

Figure 4 T-DNA insertion sites of *atmc2-1*, *atmc4-1*, and *atmc9.* Exons are indicated in black boxes.

2.2 Crossing

We used 5-6 week old plants for crossing purposes. The primary and secondary inflorescences were removed: leaves, mature flowers and siliques. Crossings were performed using fine forceps under a dissection microscope. To isolate the female acceptor, unopened flower buds were gently removed along with sepals, petals, and

stamens to leave only the immature carpel. After two days of emasculation, the mature carpel was pollinated by dabbing the stigma with a mature flower from the crossing partner. The pollinated carpels were then covered with plastic wrap to avoid pollen contamination from nearby flowers, and left to mature into siliques. The combinations of double mutants can be found in Table 1.

Table 1 *AtMC* Double Mutant Combinations

AtMC mutants abbreviation	**Double or Triple T-DNA insertion line**
atmc2/4	SALK_002986 x SAIL_856_D05
atmc4/9	SAIL_856_D05 x SALK_075814

2.3 Genomic DNA Extraction

To extract genomic DNA for genotyping, 1-2 rosette leaves were collected from the *AtMC* mutant and WT plants, and then placed into 1.5ml labeled Eppendorf tubes. The plant tissues were ground with 300µl 2X CTAB (2% Cetyltrimethylammonium bromide, 1.4M NaCl, 100 mM Tris-HCl pH8.0, 20mM EDTA) buffer, until no big chunks remained. They were then incubated at 65°C for 35 minutes to lyse the cells in order to release the DNA. After incubation, 300µl chloroform was added into the extraction buffer,

and the solution was centrifuged at full speed (13,000 rpm) for 10 minutes to separate the phases. The aqueous phase was transferred to a new tube containing 250µl isopropanol, mixed well, and incubated at room temperature for 20 minutes to precipitate DNA. After centrifuging at full speed for five minutes, the supernatant was poured away and the pellets were washed with 70% ethanol, and then centrifuged at full speed again for two minutes. Tubes were left in the hood for 20 minutes to dry out the pellets and the DNA was dissolved in 100µl of dH_2O.

2.4 Polymerase Chain Reaction (PCR) for Genotyping

PCR was used to identify the homozygous or heterozygous mutants via different primer sets (Table 2). The PCR solution mix contained 1µl genomic DNA, 1 unit ChoiceTag DNA polymerase (Denville Scientific Inc.), 1X PCR buffer with Mg^{2+}, 0.25mM dNTP (Denville Scientific Inc.)**,** 0.5µM forward primer, 0.5µM reverse primer, and added ddH_2O up to the final volume, up to the last 10µl. The PCR program used for genotyping: 94°C for three minutes, then ran for 30 cycles at 94°C for 45 sec, annealing for 30 sec at 56°C, and 50 sec elongation at 72°C. However, the annealing step of the *AtMC2* gene specific primer (GSP) set was run for 30 sec at 60°C. The final PCR step was incubated at 72°C for another five minutes to ensure the elongation process was

complete, and afterwards the products were run in 1% agarose gel and the WT or mutant alleles were identified.

Table 2 Oligonucleotide Primers for Genotyping

Primer	**Sequence 5' to 3'**	**Note**
atmc2_GSP_F	TCACGCCTTCACTCTCATCG	PCR genotyping for *atmc2-1* gene specific locus, Forward
atmc2_GSP_R	TTGGCCATCTCATTGGGTCC	PCR genotyping for *atmc2-1* gene specific locus, Reverse
EL 1626	TCGACGATGGCATGGAGCTTA	PCR genotyping for *atmc2-1* T-DNA insertion, Forward
LBa1	TGGTTCACGTAGTGGGCCATCG	PCR genotyping for *atmc2-1 and atmc9* T-DNA insertion, Reverse
EL 2336	GATAATCCGATCAGATTCAGAGAG	PCR genotyping for *atmc4-1* gene specific locus, Forward
EL 2338	CAACAACATTACATCAGCAAAGCT	PCR genotyping for *atmc4-1* gene specific locus, Reverse

EL 1526	TGTTGATGACCCTTTTGTCTTG GA	PCR genotyping for *atmc4-1* T-DNA insertion, Forward
LB3	TAGCATCTGAATTTCATAACCA ATCTCGATACAC	PCR genotyping for *atmc4-1* T-DNA insertion, Reverse
atmc9_GSP_F	TCCGAGAATTGGTCAATCAAC	PCR genotyping for *atmc9* gene specific locus and T-DNA insertion, Forward
atmc9_GSP_R	AGATTGTCATGGTCGTTCTGG	PCR genotyping for *atmc9* gene specific locus, Reverse

2.5 RNA Extraction

The total RNA was extracted from 100mg seedlings, leaf tissue of WT, or AtMC mutants using the RNeasy Plant Mini Kit (Qiagen) following the manufacturer's instructions. To avoid genomic DNA contamination, 10μg RNA was treated with a TURBO DNA-free kit (Invitrogen) and run in 1% agarose gel to determine the quality of treated samples. cDNAs were synthesized from 1.5μg DNase-treated RNA by the High-Capacity cDNA Reverse Transcription Kit (Applied Biosystems)**.**

2.6 Reverse Transcription Polymerase Chain Reaction (RT-PCR) Analysis

The first-strand cDNAs were diluted to 25ng/µl and the RT-PCR solution mix, containing 1µl cDNA (25ng/µl), ChoiceTag DNA polymerase (Denville Scientific Inc.), 1X PCR buffer with Mg^{2+}, 0.5mM dNTP (Denville Scientific Inc.), 0.25µM forward primer, 0.25µM reverse primer, was added with ddH_2O to create the final volume of 10µl. The oligonucleotide primers in this RT-PCR analysis are listed in Table 3 and the Actin2 transcript was used as the internal control. The PCR reaction was run in the following manner: 94°C for five minutes, then ran 26 or 30 cycles of 94°C for 30 sec, annealing for 30 sec at 56°C, and 30 sec elongation at 72°C. The PCR products were run in 1% agarose gel and the relative expression levels of target *AtMC* genes were analyzed.

Table 3 Oligonucleotide Primers for RT-PCR

Primer	**Sequence 5' to 3'**
atmc2-1_RT-PCR_F	TTCTTACCCGTTCACTCACGC
atmc2-1_RT-PCR_R	GGTAAGTCCATGACGGTACCAC
atmc4-1_RT-PCR_F	AGGCGGTGCTTATTGGGATCA
atmc4-1_RT-PCR_R	TCCAATGTGAAACCCTCGAGA
atmc9_RT-PCR_F	TCCAGCAACATATCTCCGGC

atmc9_RT-PCR_R	AAGCACATCCCTTGCCATCA
Actin2_RT-PCR_F	GTCTTGTTCCAGCCCTCGT
Actin2_RT-PCR_R	GAGATCCACATCTGCTGGAATG

2.7 DNA Damage Treatment

Zeocin (InvivoGen) was used as the DNA damage inducer in this study. After stratification, the WT and *AtMC* mutant seeds were grown vertically at 21°C under long day conditions (16h light and 8h dark). Four days after growing at 21°C, the seedlings were transferred to an 0.5X MS medium supplemented with 5μM or 2μM of Zeocin, and grown for an additional one to three days, and the root length was measured at the indicated time intervals by Image J software (NIH Image). The root elongation rate was calculated with the following formula:

$$\frac{(\text{DayX w/Zeocin -root length} - \text{Day0 w/Zeocin -root length})}{\text{Average (DayX MS-root length} - \text{Day0 MS-root length)}} \times 100\ (\%)$$

2.8 Propidium Iodide (PI) Staining

The root tips of Zeocin treated or non-treated seedlings were stained on the agar

surface with 5μg/ml Propidium iodide (PI) for three minutes at room temperature, and then transferred to water, pre-wetted microscope slides. The images were taken using an Olympus FSX100 all-in-one fluorescence microscope.

2.9 Quantitative Real-Time PCR (qRT-PCR) Analysis

The total RNA was extracted from the 0.5 cm root tips of 5μM Zeocin treated WT plants. The RNA extraction and cDNA synthesis method were as described before. The qRT-PCR was performed with a 25μl reaction solution, containing 1μl diluted- cDNA (25ng/μl), 12.5μl Power SYBR Green Master Mix (Applied Biosystems), 1 μl forward qRT-PCR primer, 1 μl reverse qRT-PCR primer, and 9.5μl ddH_2O using the StepOnePlus PCR system (Applied Biosystems) under the following conditions: 50°C for two minutes, 95°C for 10 minutes, then ran 40 PCR cycles at 94°C for 15 sec and 60°C for one minute. The oligonucleotide primers in this qRT-PCR analysis are listed in Table 4 and the Actin2 transcript was used as the internal control (Czechowski et al. 2005). The comparative ΔΔCT method (User Bulletin #2: Relative Quantitation of Gene Expression, Applied Biosystems) was used to calculate and analyze the result of qRT-PCR.

Table 4 Oligonucleotide Primers for qRT-PCR

Primer	**Sequence 5' to 3'**
atmc4-1_qRT-PCR_F	TGCAGACACACGTTGGGAGTA
atmc4-1_qRT-PCR_R	GCGGAACCGAACCTCTTGA
atmc9_qRT-PCR_F	TGACGGCCCGTGAAAAA
atmc9_qRT-PCR_R	CCTGACACCCGCTCATCAA
ACT2_qRT-PCR_F	CTTGCACCAAGCAGCATGAA
ACT2_qRT-PCR_R	CCGATCCAGACACTGTACTTCCTT

3. Results

3.1 Characterization of AtMC mutants

All of the single and double mutants were genotyped as homozygous mutations (Fig. 4) and analyzed for the effect of T-DNA insertion by RT-PCR (Fig. 5). According to the results, we confirmed the single and double mutant lines used in this study are gene knockout mutants.

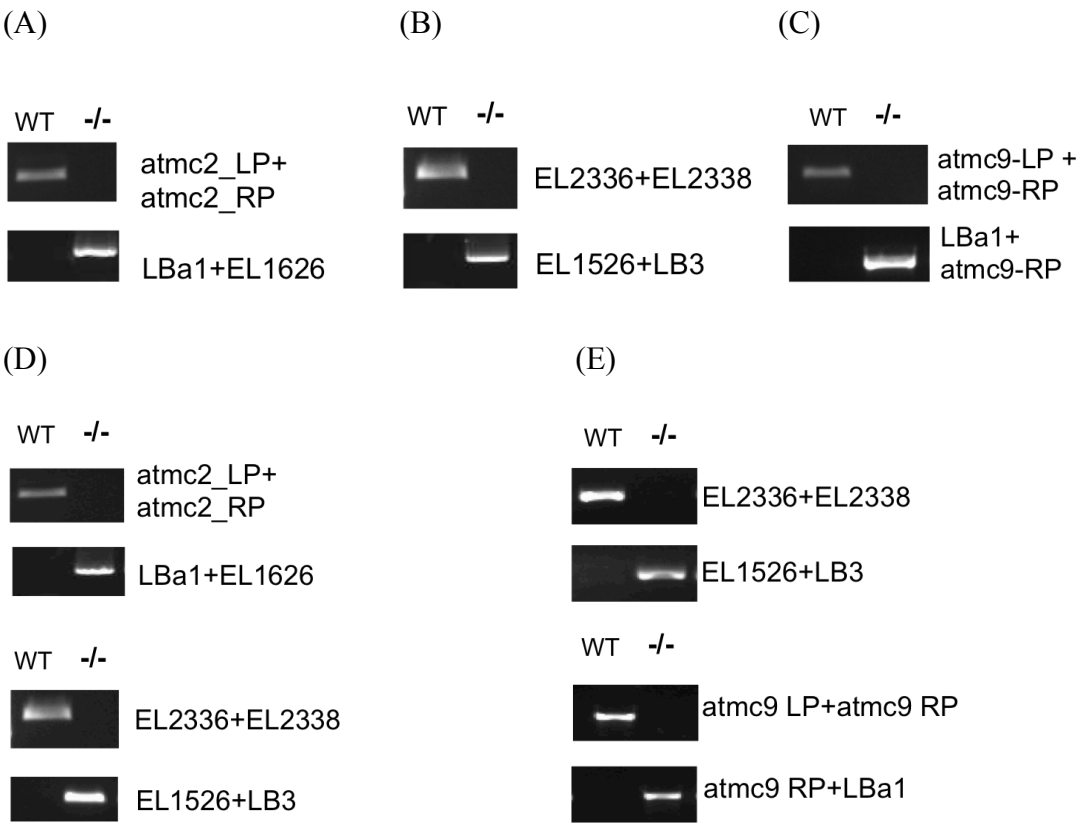

Figure 5 Genotyping analysis of AtMC mutants. (A) *atmc2-1*. (B) *atmc4-1*. (C) *atmc9*. (D) *atmc2/4*. (E) *atmc4/9*.

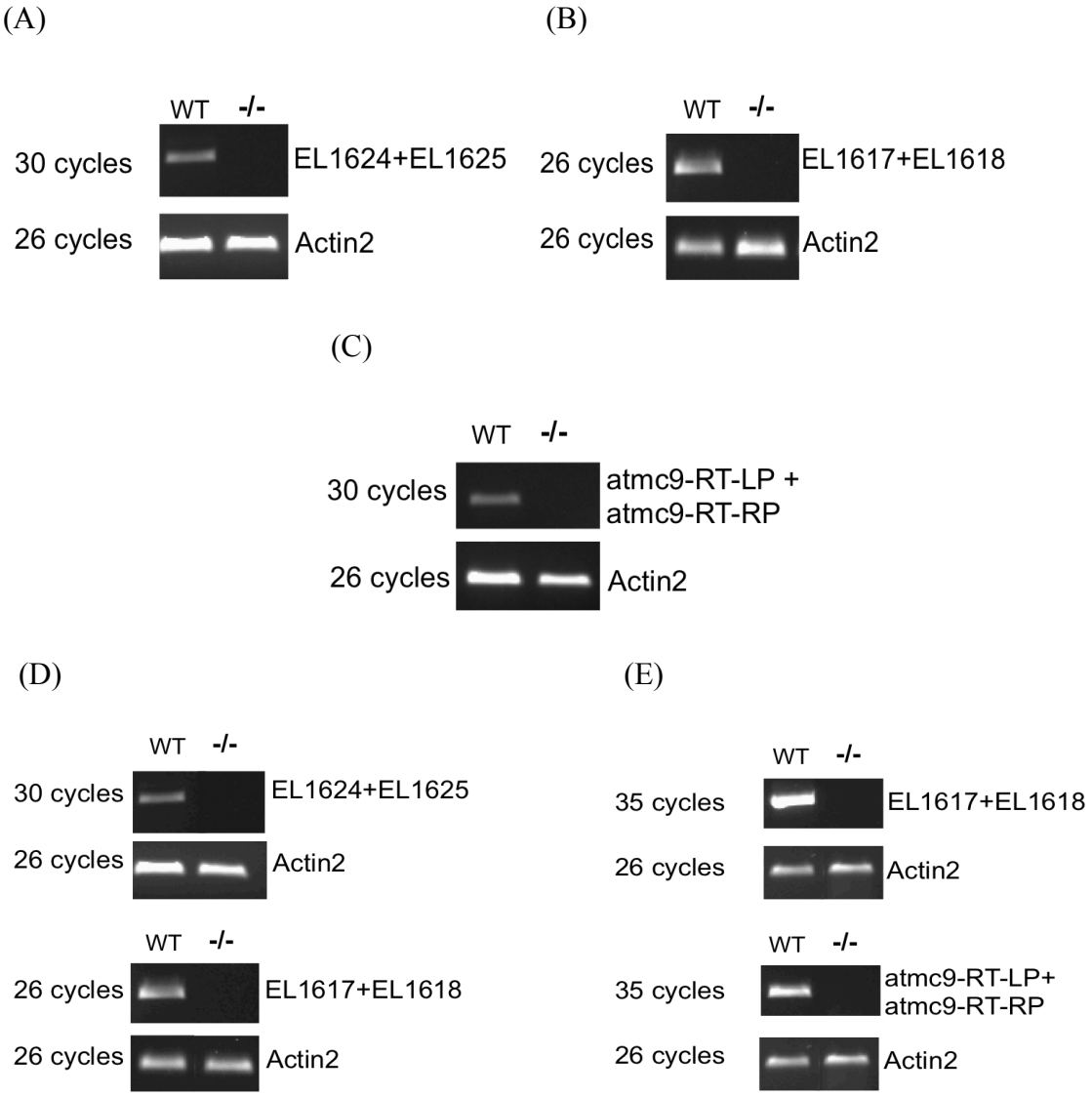

Figure 6 RT-PCR analysis of AtMC mutants. (A) *atmc2-1*. (B) *atmc4-1*. (C) *atmc9*. (D) *atmc2/4*. (E) *atmc4/9*.

3.2 DNA Damage Treatment

3.2.1 Zeocin Inhibits Root Growth in WT and AtMCs Mutants

In order to determine the function of AtMCs in DNA damage induced-root elongation arrest , we used *AtMC2* (a negative regulator in pathogen-induced PCD), *AtMC4* (which is abundantly expressed in all tissues) and *AtMC9* (with its unique structure and the expression highly localized in the root tip area) as our target genes. Five to six days old AtMC single (*atmc2-1*, *atmc4-1*, *atmc9*) and double (*atmc2/4* and *atmc4/9*) mutant seedlings were used in this experiment.

Zeocin was used as the DNA damage inducer in this study. The working reagent is a copper-chelated glycopeptide antibiotic. After it entered the cells, Zeocin was activated due to the copper cation reduction (Cu^{2+} to Cu^{+}). Once it is activated, Zeocin bound to DNA and cleavage occur, then causing cell death (Berdy, 1980).

After 5μM or 2μM of Zeocin treatments, both *atmc2-1*, *atmc4-1* and *atmc2/4* had a higher root elongation rate than WT plants (Fig. 6) at the early time interval. However, the *atmc2/4* double mutants did not show a significant additive effect compared to the single AtMC mutants using the root elongation assay.

We also tested two different Type II AtMC genes with the Zeocin treatment. It was discovered that the *atmc9* single and *atmc4/9* double mutants dramatically inhibited root

elongation arrest (Fig. 7), and the phenotypes had significant differences at 2μM of Zeocin (Fig. 8). Despite the inhibition of root elongation in *atmc4-1,* and that *atmc9* was lower than WT plants, *atmc4/9* double mutants had no additive effect and are similar to *atmc9* alone (Fig. 7).

The root elongation rate of *atmc4-1* in two experiment is slightly different (Fig. 6 and Fig. 7). The reason for this difference might be the phytagel source. A different phytal gel source may result in adventitious root formation, and may affect the result of the root elongation rate; however, the effect of Zeocin in *atmc 4-1* and WT plants at the early time interval was similar in these two experiments, thus we conclude that *AtMC4* was consistently found to be involved as a positive factor in the Zeocin-induced root elongation arrest.

Zeocin treatment not only inhibits root elongation, but also leads to root tip disorganization (Fig. 9). We determined the root tip disorganization by calculating the number of disorganized root tip structure divided by the total number of Zeocin-treated roots per replicates (%). There was no significant difference in terms of the root tip disorganization ratio between WT plants, *atmc2-1*, *atmc4-1*, and *atmc2/4* at three days after 5μM of Zeocin treatment (Fig. 9). In contrast, both *atmc9* and *atmc4/9* mutants had dramatically inhibited root tip disorganization (Fig. 10). These results show that *AtMC9*

plays a critical role for the Zeocin-induced root growth arrest process, which works upstream of *AtMC4*.

Since *atmc 9* mutants had a strong phenotype in the root tip after Zeocin treatment, we used two Type II AtMC single and double mutants (*atm c4-1, atmc 9*, and *atmc 4/9*) as the material for subsequent experiments.

(A)

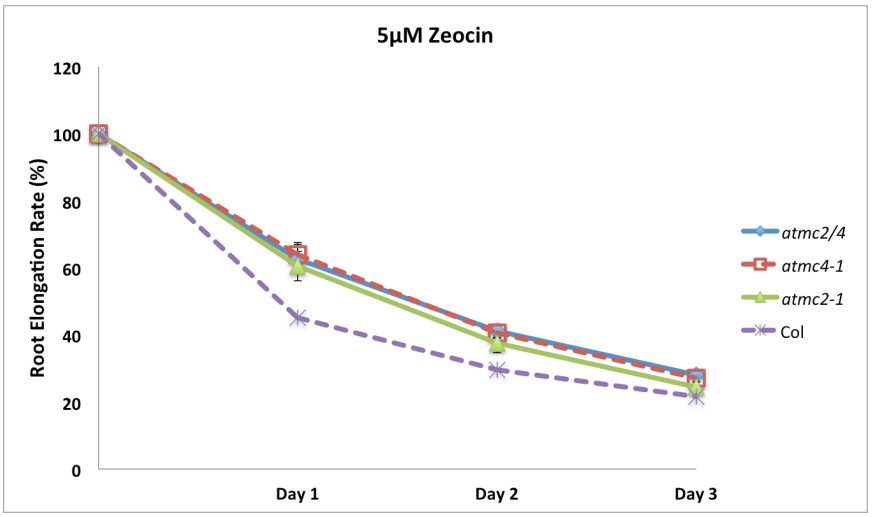

(B)

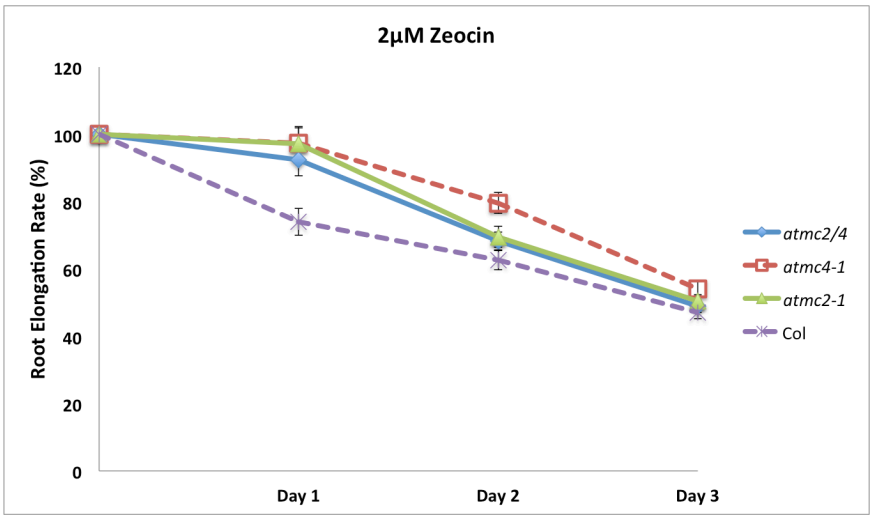

Figure 7 Effects of Zeocin treatment on primary root elongation of Type I (*AtMC2*) and Type II (*AtMC4*) *AtMC* knockout mutants. (A) 5μM. (B) 2μM. Each value represents the mean ± SE of 21 seedlings per genotype per time, and the result was confirmed by two independent experiments. Asterisks indicate significant differences form WT plants with Student's *t*-values (**P < 0.001, *P< 0.05).

(A)

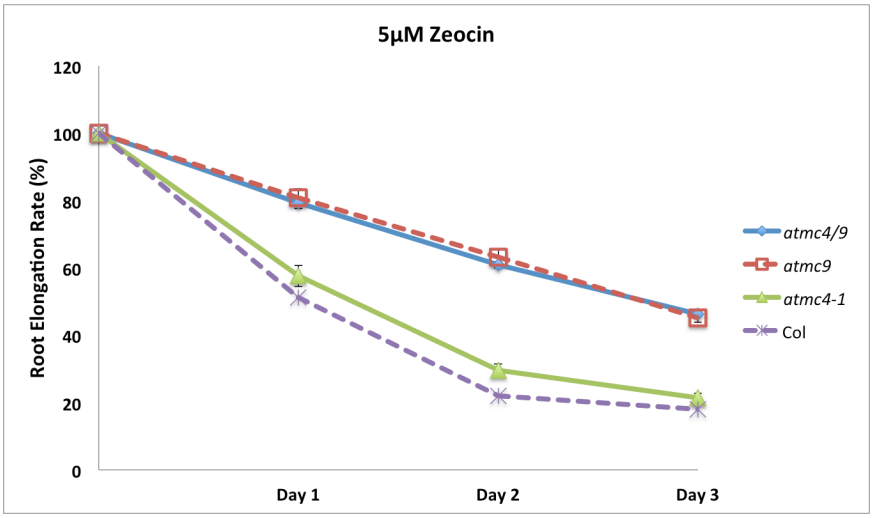

(B)

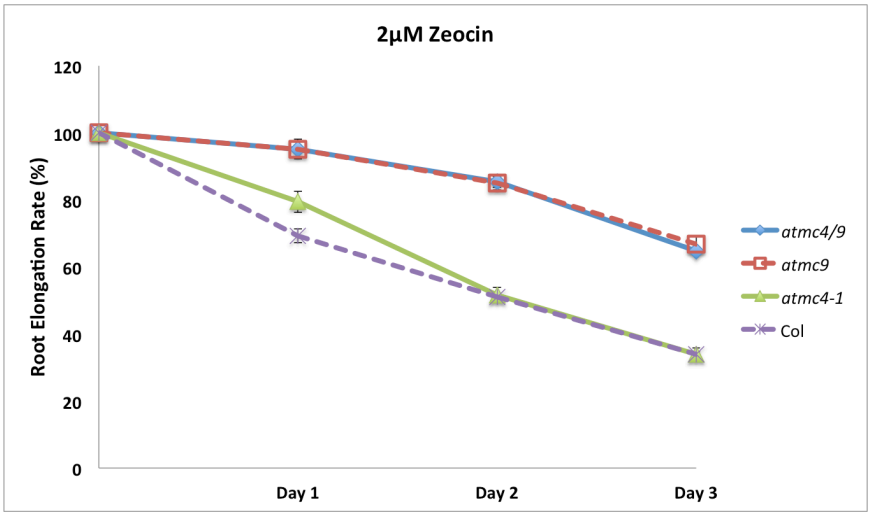

Figure 8 Effects of Zeocin treatment on primary root elongation of Type II AtMC (*AtMC4* and *AtMC9*) knockout mutants. (A) 5μM. (B) 2μM. Each value represents the mean ± SE of 35 seedlings per genotype per time, and the result was confirmed by two independent experiments. Asterisks indicate significant differences form WT plants with Student's *t*-values (**P < 0.001, *P< 0.05).

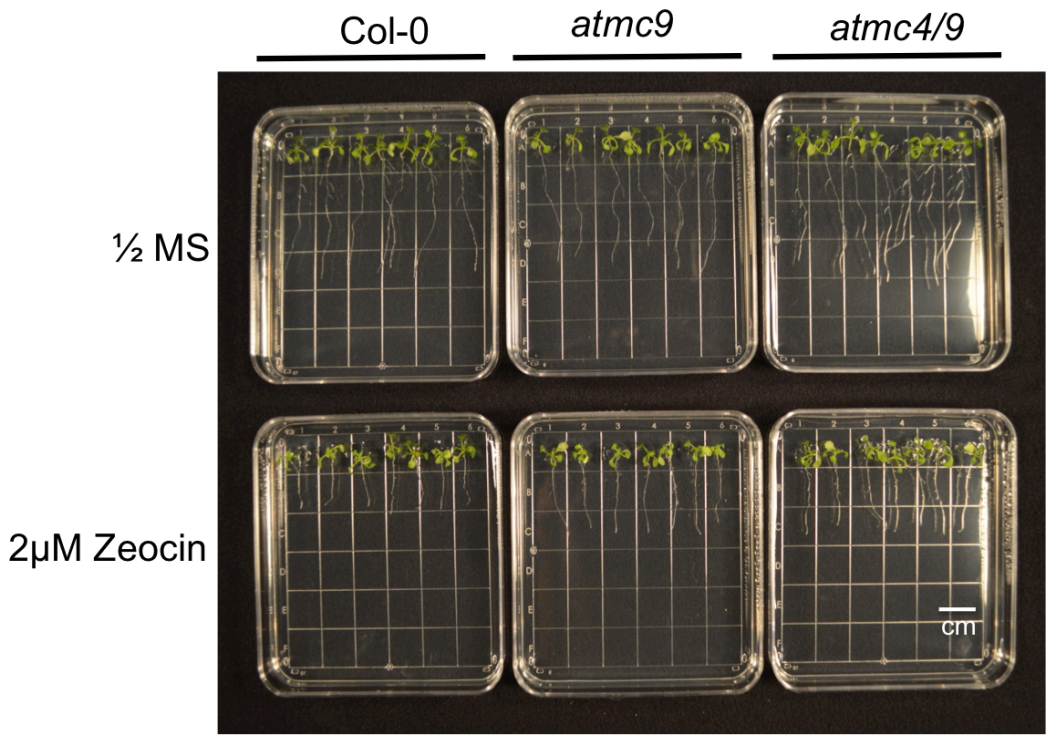

Figure 9 The phenotypical result of different genetic backgrounds at seven days after 2μM of Zeocin treatment.

(A)

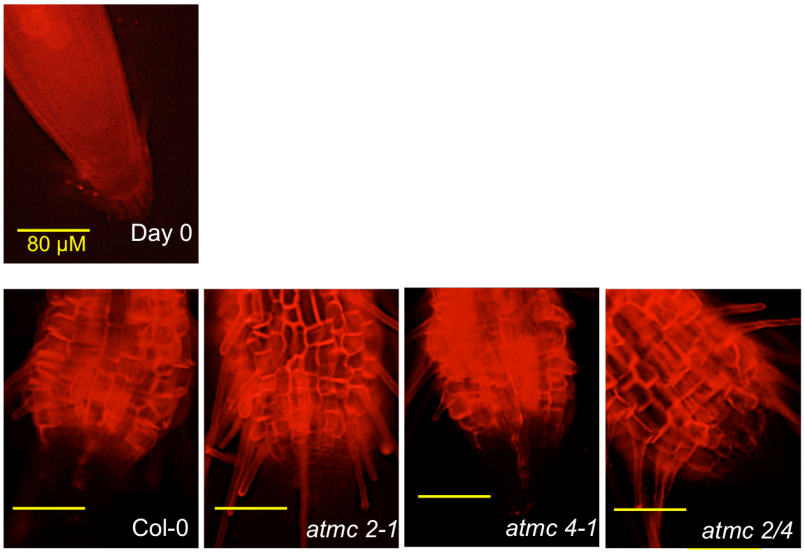

(B)

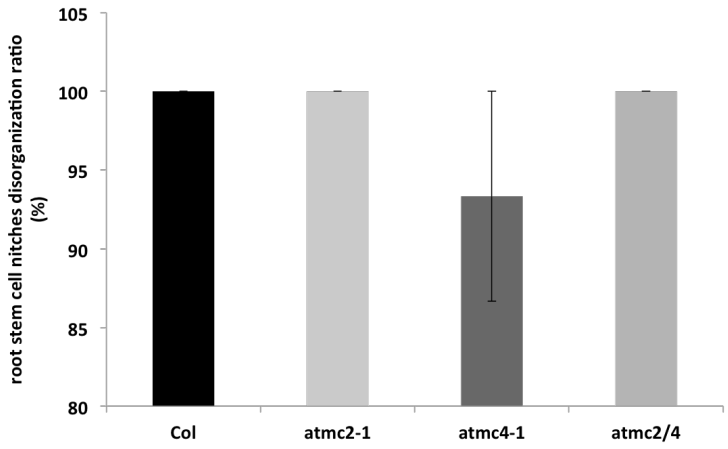

Figure 10 Zeocin-induced root tip region disorganization of *atmc2-1*, *atm 4-1*, and the *atmc2/4* mutants. (A) After three days of 5μM of Zeocin treatment, root tip disorganization could be found in different genetic backgrounds. (B) Zeocin-induced root tip disorganization at three days after transferring to the MS media with 5μM of Zeocin. Each value represents the mean ± SE of three replicates (five seedlings for each).

(A)

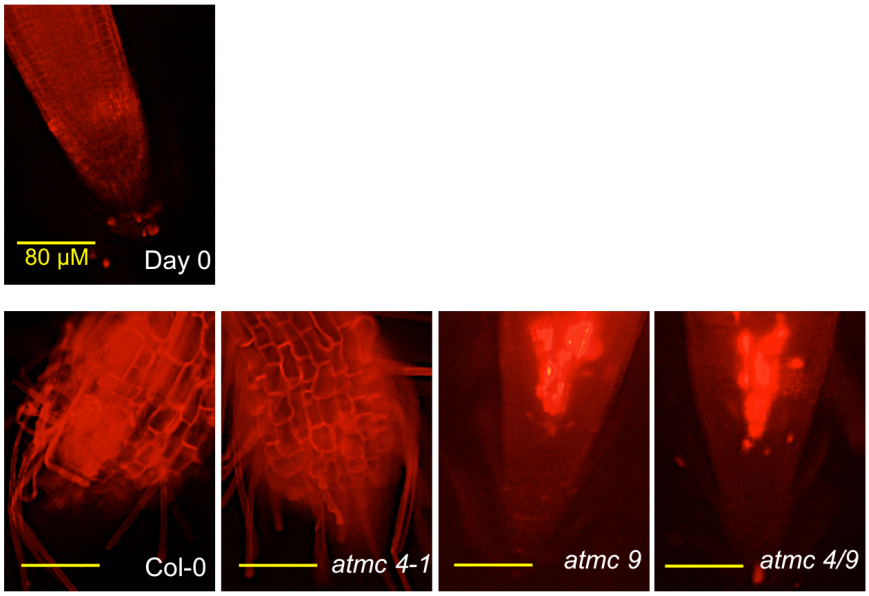

(B)

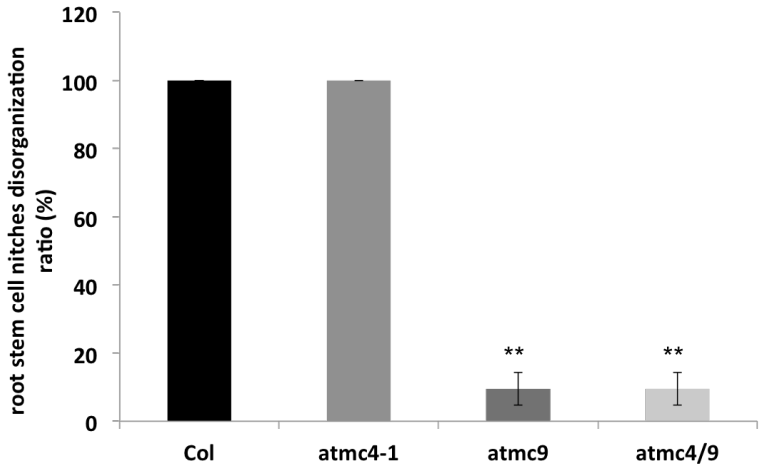

Figure 11 Zeocin-induced root tip region disorganization of *atmc4-1*, *atmc9*, and the *atmc4/9* mutants. (A) After three days of 5μM of Zeocin treatment, root tip disorganization could be found in different genetic backgrounds. (B) Zeocin-induced root tip disorganization at three days after transferring to the MS media with 5μM of Zeocin.

Each value represents the mean ± SE of three replicates (seven seedlings for each). Asterisks indicate significant differences from WT plants with Student's t-values (** $P < 0.001$).

3.2.2 AtMCs Involved in Zeocin-Treated Stem Cell Death Process.

Recent publications indicated that Zeocin-induced PCD in root stem cell niches (Fulcher and Sablowski, 2009; Furukawa et al., 2010). In order to determine the function of *AtMC* genes in Zeocin-induced stem cell death process, six days old *atmc4-1*, *atmc9* and *atmc4/9* seedlings were used for the materials. Propidium iodide (PI) can penetrate dead cells while live cells exclude it, so we used PI to determine the level of the cell death process by measuring the intensely PI-stained area.

After 24h of 5μM of Zeocin treatment, there was no significant difference of cell death area between WT plants and *atmc4-1* mutants (Fig. 11); however, a dramatic suppression of root stem cell death was seen in *atmc9* and *atmc4/9* mutants. Unlike previous results, *atmc4/9* double mutants have the lowest cell death level compared to other genetic backgrounds (Fig. 11B). This result shows that *AtMC4* and *AtMC9* might work additively in Zeocin-induced PCD, but not in the root elongation arrest process.

(A)

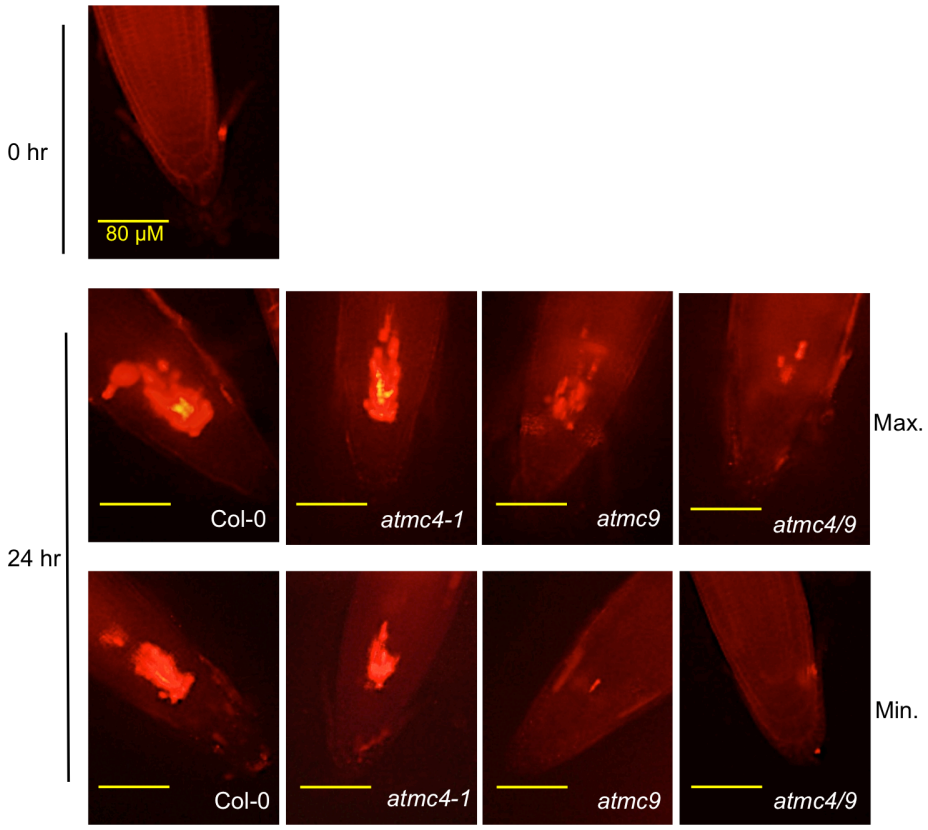

(B)

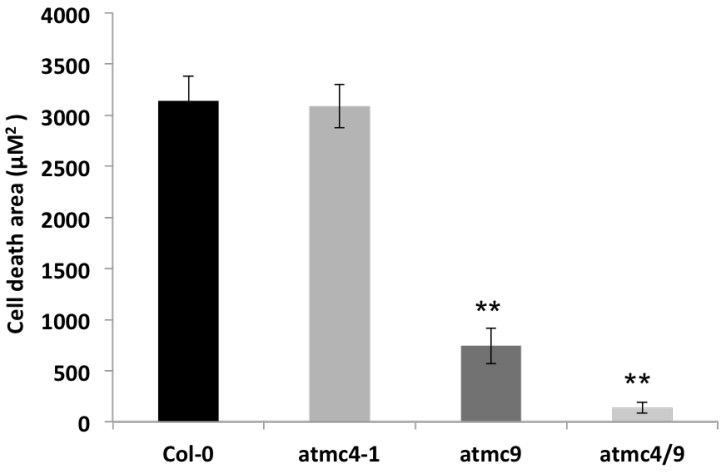

Figure 12 Zeocin-induced stem cell death of *atmc4-1*, *atmc9*, and the *atmc4/9* mutants.

(A) 5μM of Zeocin-induced cell death in different genetic backgrounds. The maximum and minimum of dead cells (intensely PI-stained) areas were shown above. (B) Zeocin-induced stem cell death at 24 h after transferring to the MS media with 5μM of Zeocin. Each value represents the mean ± SE of three replicates (seven seedlings for each). Asterisks indicate significant differences from WT plants with Student's t-values (** $P < 0.001$).

3.2.3 Zeocin Induced the Expression of AtMC4 and AtMC9 Genes.

In order to analyze the AtMC's gene expression after Zeocin treatment, we first tested the WT root stem cell death occurrence time interval. The PCD occur rate was calculated by the number of root tips that can be observed significant intensely PI-stained area divided by the total number of Zeocin-treated roots per replicates (%).

According to the result of Fig. 12, the dead root stem cell (indicated by the intensity of PI-stain) can be observed as early as eight hours after transfer to the Zeocin plate, and 100% of the root tips had undergone the PCD process after 16 h. The results clearly indicate that the PCD pathway is activated within eight hours after DNA damage treatment.

Based on the previous results, we collected the Zeocin-treated root tip region at eight hours and sixteen hours. *AtMC4* transcription level dramatically increased after the Zeocin treatment (Fig. 13A). The expression level of *AtMC9* was significantly lower than *AtMC4*, however, a lesser but still significant induction of *AtMC9* can be observed after the Zeocin treatment (Fig. 13B). Taken together, we concluded that Zeocin upregulated the expression of *AtMC4* and *AtMC9*.

(A)

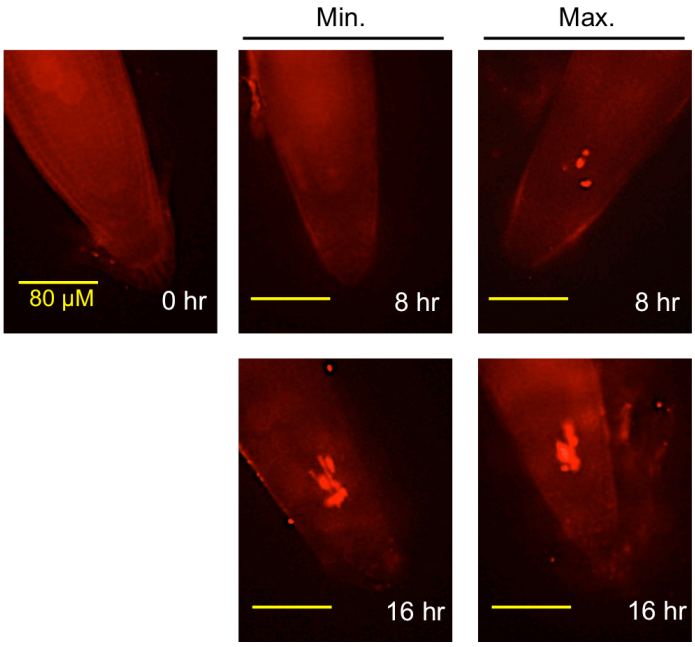

(B)

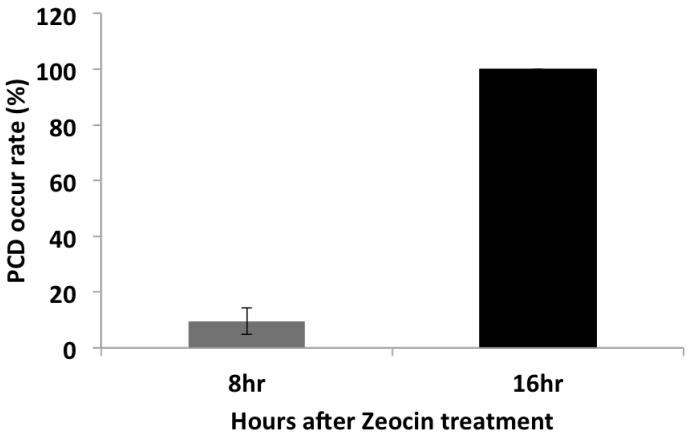

Figure 13 5μM Zeocin-induced cell death process within 24 hr. (A) The maximum and minimum dead cells (intensely PI-stained) areas at different time intervals. (B) The quantitative data of PCD occurrence time intervals. Each value represents the mean ± SE of three replicates (seven seedlings for each).

(A)

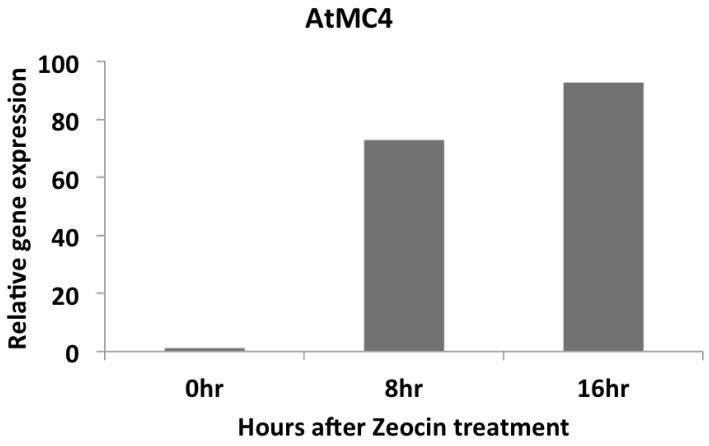

(B)

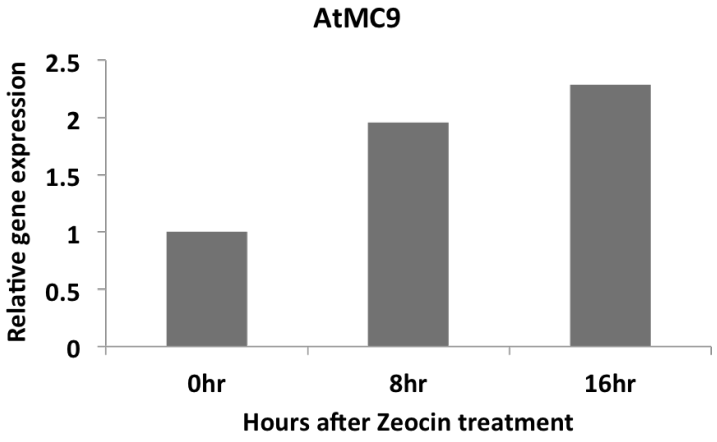

Figure 14 Expression patterns of *AtMC* genes in response to the Zeocin treatment. (A) *AtMC4*. (B) *AtMC9*. Six-day-old WT Col-0 seedlings were treated with 5μM of Zeocin, and the root tips were collected at indicated time points. The data was confirmed by two independent samples.

4. Discussion and future work

Genomic DNA is exposed to internal and external stresses every day that trigger DNA damage responses. To maintain the integrity of the genome, living organisms induce different downstream consequences, like DNA repair mechanisms, cell-cycle arrest, or apoptosis. In animals, the stem cells have a lower resistance to DNA damage, which leads to p53-dependant apoptosis (Rich et al., 2000). This selective cell death protection mechanism was also discovered in plants, and it is an efficient way to remove the damaged cells in a shorter time frame. Recent reports demonstrated that the damage from DNA stress causes shoot or root stem cell death (Fulcher and Sablowski, 2009; Furukawa et al., 2010). The results of this study are consistent with the previous reports that DNA damage-induced cell death was initiated in root stem cell niches, and was triggered within eight hours after the Zeocin treatment (Fig. 12).

DNA damage-induced programmed root stem cell death is activated by plant specific transcription factor SOG1, and also requires either ATM or ATR (Fulcher and Sablowski, 2009; Furukawa et al., 2010). Furukawa et al. reports that *sog1-1* mutants have a high suppression of root stem cell death at 24 h after 80 Gy radiation. *AtMC*s mutants, especially *atmc9* and *atmc4/9* double mutants had lower PCD levels after the Zeocin treatment, however, they cannot inhibit PCD occurrence in the stem cell niches at

the early time interval (Fig. 11). It indicates that AtMCs are involved in DNA damage-induced stem cell death and are up-regulated by the SOG1 transcription factor. Sablowski et al. (2009) reported that the *atmc8-1* mutant did not affect Zeocin-induced cell death of the root tip area. *AtMC8* is a positive regulator in plant oxidative-induced PCD (He et al., 2008). This study's data strongly demonstrates that *AtMC9* plays a positive regulatory role in this type of PCD (Fig. 10.11). One possible explanation could be that different AtMCs may have one specific working pathway, and this preference might not have redundancy. This can also describe *AtMC2*, a negative regulator in pathogen-induced PCD, which works as a positive function at the early time interval in Zeocin-induced PCD (Fig. 6).

According to the result of AtMC's promoter GUS fusion analysis, *AtMC9* is highly expressed in root cap cells and in developing xylem vessels (Bollhöner et al., 2013; Tsiatsiani et al., 2013). This evidence support that the *atmc9* mutant had dramatic suppression of primary root elongation arrest and the cell death level was reduced after the Zeocin treatment (Fig. 7, 8, and 10). However, the effect of AtMCs in root elongation and the cell death process might not be the same.

AtMC5 has a highly similar sequence to AtMC4, and the locus locations are close to each other (Fig. 1), so the function of AtMC5 may be redundant to AtMC4. AtMC's

promoter GUS fusion analysis indicated that *AtMC4* was abundantly expressed in whole plant tissue. The GUS expression of *AtMC5* was similar to *AtMC4* but was overall weak (Kwon and Hwang, 2013); however, *AtMC5* was ubiquitously expressed in root elongation zone tissue (Bollhöner et al., 2013). These results are explained by the fact that the *atmc4/9* mutant had a significant reduction in cell death level instead of root elongation rate.

The number of AtMC genes in the genome is varies in different species (Tsiatsiani et al., 2011; Fagundes et al., 2015). However, based on the BLAST result in Inparanoid (http://inparanoid.sbc.su.se/cgi-bin/index.cgi) and MEROPS peptidase database (http://merops.sanger.ac.uk), AtMC4 and AtMC9 are the only two highly conserved Type II metacaspases in Plantae, such as: *Solanum lycopersicum*, *Oryza sativa* (Huang et al., 2015), *Vitis vinifera,* or duckweed (Lam lab, unpublished data). These results indicate that AtMC4 and AtMC9 are the essential genes in Plantae.

Confirming the function of AtMC9 in DNA damage-induced PCD will be the most important thing for further study. We plan to use other putative *atmc9* T-DNA knockout mutants, or use complimentary strategy, which will overexpress *AtMC9* in *atmc9* or *atmc4/9* double mutant background.

Second, understanding the distribution area of DNA damage within different cells

will help us to clarify the Zeocin-activated PCD pathway. It is important to determine the DNA damage level in stem cells of *atmc9* mutant and WT in different time points. What is the final fate of the damaged-DNA? Do *atmc9* mutants have higher DNA recovering mechanism than WT? Terminal deoxynucleotidyl transferase (TdT) dUTP Nick-End Labeling assay (TUNEL assay), a common method to detect the cells which undergoing PCD process, would be the best strategy. TdT enzyme can catalyze the dUTPs then bind to the 3'-OH site of double-strand break DNA. Detecting the fluorescence carried by the enzyme can be used to determine the DNA damage distribution.

Third, previous studies indicate that plant specific transcription factor SOG1 plays crucial role in DNA damage response (Yoshiyama et al., 2009; Yoshiyama et al., 2013). However, the pathway of SOG1 and downstream PCD process is still unknown. Analyzing the gene expression level of *AtMC*s in sog1 mutation background is a key can help us to understand the function of AtMCs in SOG1-mediated DDR pathway.

5. Conclusion

In conclusion, the putative model pathways of *AtMC*s in DNA damage-induced root stem cell PCD is shown below. *AtMC2*, which is known as a negative regulator in pathogen-induced PCD, may have different functions in response to different stress, which works as a positive regulator in Zeocin-induced root elongation arrest. Furthermore, both *AtMC4* and *AtMC9* positively regulate PCD level and *AtMC9* plays a critical role for the Zeocin-induced root growth arrest process, which works upstream of *AtMC4*.

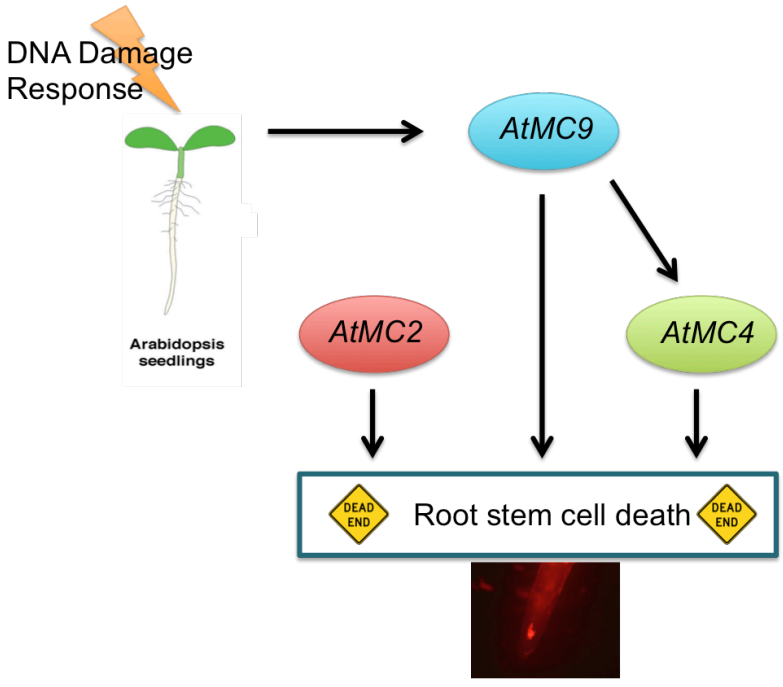

Figure 15 Putative model pathways of *AtMC*s in Zeocin-activated *Arabidopsis* root stem PCD process.

6. Reference

Adachi, S., Minamisawa, K., Okushima, Y., Inagaki, S., Yoshiyama, K., Kondou, Y., Kaminuma, E., Kawashima, M., Toyoda, T., Matsui, M., Kurihara, D., Matsunaga, S., & Umeda, M. (2011). Programmed induction of endoreduplication by DNA double-strand breaks in *Arabidopsis*. Proc. Natl. Acad. Sci. 108, 10004-10009.

Andersen, M. H., Becker, J. C., & Straten P. (2005). Regulators of apoptosis: suitable targets for immune therapy of cancer. Nat. Rev. Drug Discov. 4, 399-409.

Benneau, L., Ge, Y., Drury. G. E., & Gallois, P. (2008). What happened to plant caspases? J. Exp. Bot. 59, 491-499.

Berdy, J. 1980. Bleomycin-type antibiotics. In Amino Acid and Peptide Antibiotics. Handbook of Antibiotic Compounds, IV (1). Edited by J. Berdy. Boca Raton, FL: CRC Press.

Bollhöner, B., Zhang, B., Stael, S., Denancé, N., Overmyer. K., Goffner. D., Van Breusegem, F. & Tuominen, H. (2013). *Post mortem* function of AtMC9 in xylem vessel elements. New Phytol. 200, 498-510.

Bonneau, L., Ge, Y., Drury, G. E., & Gallois, P. (2008). What happened to plant caspases? J. Exp. Bot. 59, 491-499.

Bozhkov, P. V. & Lam, E. (2011). Green death: revealing programmed cell death in plants. Cell Death Differ. 18, 1239–1240.

Bozhkov, P. V., Suarez, M. F., Filonova, L. H., Daniel, G., Zamyatnin, A. A., Rodriguez-Nieto, S., Zhivotovsky, B., & Smertenko A. (2005). Cysteine protease mcII-PA executes programmed cell death during plant embryogenesis. Proc. Natl. Acad. Sci. 102, 14463-14468.

Cambra, I., Garcia, F. J., & Martinez, M. (2010). Clan CD of cysteine peptidases as an example of evolutionary divergences in related protein families across plant clades. Gene. 449, 59-69.

Castillo-Olamendi L., Bravo-Garc. A. A, Mor. n J., Rocha-Sosa, M., & Porta H. 2007. *AtMCP1b*, a chloroplast-localised metacaspase, is induced in vascular tissue after wounding or pathogen infection. Funct. Plant Biol. 34, 1061-1071.

Ciccia, A. & Elledge, S. J. (2010). The DNA damage response: making it safe to play with knives. Mol. Cell 40, 179-204.

Cimprich, K. A. & Cortez, D. (2008). ATR: An essential regulator of genome integrity. Nat. Rev. Mol. Cell Biol. 9, 616–627.

Cohen, G. M. (1997). Caspases: the executioners of apoptosis. Biochem. J. 326, 1-16.

Coll N. S., Epple P., and Dangl J. L. (2011). Programmed cell death in the plant immune system. Cell Death Differ. 18: 1247-1256.

Coll, N. S., Smidler, A., Puigvert, M., Popa, C., Valls, M., & Dangl, J. L. (2014). The plant metacaspase AtMC1 in pathogen-triggered programmed cell death and aging: functional linkage with autophagy. Cell death Differ. 21, 1399-1408.

Coll, N. S., Vercammen, D., Smidler, A., Clover, C., Van Breusegem, F., Dangl, J. L., & Epple, P. (2010). *Arabidopsis* type Ⅰ metacaspases control cell death. Science 330, 1393-1397.

Czechowski, T., Stitt, M., Altmann, T., Udvardi, M., & Scheible W. (2005). Genome-wide identification and testing of superior reference genes for transcript normalization in *Arabidopsis*. Plant Physiol. 139, 5-17.

Fagundes, D., Bohn, B., Cabreira, C., Leipelt, F., Dias, N., Bodanese-Zanettini, M.H., & Cagliari, A. 2015. Caspases in plants: metacaspase gene family in plant stress responses. Funct. Integr. Genomics 15, 639-649.

Fulcher, N. & Sablowski, R. (2009). Hypersensitive to DNA damage in plant stem cell niches. Proc. Natl. Acad. Sci. 106, 20984-20988.

Furukawa, T., Curits, M. J., Tominey. C. M., Duong. Y. H., Wilcox. B. W. L., Aggoune, D., Hays, J. B., and Britt. A. B. (2010). A shared DNA-damage-response pathway for induction of stem-cell death by UVB and by gamma irradiation. DNA Repair 9, 940-948.

Garcia, V., Brunchet, H., Camescasse, D., Granier, F., Bouchez, D., & Tissier, A. (2003). *AtATM* is essential for meiosis and the somatic response to DNA damage in plants. Plant Cell 15, 119-132.

He, R., Drury, G. E., Rotari, V. I., Gordon, A., Willer, M., Farzaneh, T., Woltering, E.J., & Gallois, P. (2008). Metacaspase-8 modulates programmed cell death induced by ultraviolet light and H_2O_2 in *Arabidopsis*. J. Biol. Chem. 283, 774-783.

Helton, E. S. and Chen, X. (2007). p53 modulation of the DNA damage response. J. Cell. Biochem.100, 883-896.

Huang, L., Zhang, H., Hong, Y., Liu, S., Li, D., & Song, F. (2015). Stress-responsive expression, subcellular localization and protein-protein interactions of the rice metacaspase family. Int. J. Mol. Sci. 16, 16216-16241.

Kim, S. M., Bae, C., Oh, S. K., & Choi, D. (2013). A pepper (*Capsicum annuum* L.) matacaspase 9 (*Camc9*) plays a role in pathogen-induced cell death in plant. Mol. Plant Pathol. 14, 557-566.

Kwon, S. I. & Hwang, D. J. (2013). Expression analysis of the metacaspase gene family in *Arabidopsis*. J. Plant Biol. 56, 391-398.

Lam, E. (2004). Controlled cell death, plant survival and development. Nature Rev. Mol. Cell Biol. 5, 305-315.

Lam, E. & Zhang, Y. (2012). Regulating the reapers- Activating metacaspases for programmed cell death. Trends in Plant Sci. 17, 487-494.

Madeo, F., Herker, E., Maldener, C., Wissing, S., Lächelt, S., Herlan, M., Fehr, M., Lauber, K., Sigrist, S. J., Wesselborg, S., & Fröhlich, K. (2002). A caspase-related protease regulates apoptosis in yeast. Mol. Cell 9, 911-917.

Ohashi-Ito, K., Oda, Y., & Fukuda, H. (2010). *Arabidopsis* VASCULAR-RELATED NAC-DOMAIN6 directly regulates the genes that govern programmed cell death and secondary wall formation during xylem differentiation. Plant Cell 22, 3461–3473.

Rich, T., Allen, R. L., & Wyllie, A. H. (2000). Defying death after DNA damage. Nature 407, 777-783.

Shiloh, Y. (2006) The ATM-mediated DNA-damage response: Taking shape. Trends Biochem. Sci. 31, 402–410.

Tait, S. W. G. & Green, D.R. (2010). Mitochondria and cell death: outer membrane permeabilization and beyond. Nat. Rev. Mol. Cell Biol. 11, 621-632.

Tsiatsiani, L., Timmerman, E., De Bock, R. J., Vercammen, D., Stael, S., van de Cotte, B., Staes, A., Goethals, M., Beunens, T., Damme, P. V., Gevaert, K., & Breusegem, F. V. (2013). The *Arabidopsis* METACASEPASE9 degradome. Plant Cell 25, 2831 2847.

Tsiatsiani, L., Van Breusegem, F., Gallois, P., Lam, E., & Bozhkov, P. V. (2011). Metacspase. Cell Death Differ. 18, 1279-1288.

Turner, S., Gallois, P., & Brown, D. (2007). Tracheary element differentiation. Annu. Rev. Plant Biol. 58, 407–433.

Uren, A. G., O'Rourke, K., Aravind, L., Pisabarro, M. T., Seshagiri, S., Koonin, E. V., & Dixit, V. M. (2000). Identification of paracaspases and metacaspases: two ancient families of caspase-like proteins, one of which plays a key role in MALT lymphoma. Mol. Cell 6, 961-967.

Uren, A. G., O'Rourke, K., Aravind, L., Pisabarro, M. T., Seshagiri, S., Koonin, E.V., & Dixit, V. M. (2000). Identification of paracaspases and metacaspases: two ancient families of caspase-like proteins, one of which plays a key role in MALT lymphoma. Mol. Cell 6:961-967.

van Baarlen, P., Woltering, E. J., & Staats, M. (2007). Histochemical and genetic analysis of host and non-host interactions of *Arabidopsis* with three Botrytis species: an important role for cell death control. Mol. Plant Pathol. 8, 41-54.

Vercammen, D., Belenghi, B., van de Cotte, B., Beunens, T., Gavigan, J. A., De Rycke,

R., Brackenier, A., Inz, D., Harris, J. L., & Van Breusegem, F. (2006). Serpin1 of *Arabidopsis thaliana* is a Suicide Inhibitor for Metacaspase 9. J. Mol. Biol. 364, 625-636.

Vercammen, D., Declercq, W., Vandenabeele, P., & Breusegem, F. V. (2007). Are metacaspases caspases? J. Cell Biol. 179, 375-380.

Vercammen, D., van de Cotte, B., Jaeger, G. D., Eeckhout, D., Casteel, P., Vandepoele, K., Vandenberghe, I., Van Beemen, J., Inzé, D., & Van Breusegem, F. (2004). Type II metacaspases Atmc4 and Atmc9 of *Arabidopsis thaliana* cleave substrates after arginine and lysine. J. Bio. Chem. 279, 45329-45336.

Watanabe, N. & Lam E. (2005). Two *Arabidopsis* metacaspases AtMCP1b and AtMCP2b are arginine/lysine-specific cysteine protease and activate apoptosis-like cell death in yeast. J. Biol. Chem. 280, 14691-14699.

Watanabe, N. & Lam, E. (2004). Recent Advance in the study of caspase-like proteases and Bax inhibitor-1 in plants: their possible roles as regulator of programmed cell death. Mol. Plant Pathol. 5, 65-70.

Watanabe, N. & Lam, E. (2011). *Arabidopsis* metacaspase 2d is a positive mediator of cell death included during biotic and abiotic stresses. Plant J. 66, 969-982.

Watanabe, N. and Lam E. (2011). Calcium-dependent activation and autolysis of *Arabidopsis* metacaspase 2d. J. Biol. Chem. 286, 10027-10040.

Woltering, E. J. (2004). Death proteases come alive. Trends Plant Sci. 9, 469-472.

Yoshiyama, K. O., Kimura. S., Maki, H., Britt, A. B., & Umeda, M. (2014). The role of SOG1, a plant-specific transcriptional regulator, in the DNA damage response. Plant Signaling Behav. 9, e28889_1-8.

Yoshiyama, K. O., Sakaguchi, K., & Kimura, S. (2013). DNA damage response in plant: conserved and variable response compared to animals. Biology 2, 1338 1356.

Yoshiyama, K.; Conklin. P. A., Huefner, N. D., & Britt, A.B. (2009). Suppressor of gamma response 1 (*sog1*) encodes a putative transcription factor governing multiple responses to DNA damage. Proc. Natl. Acad. Sci. 106, 12843-12848.

Zimmermann, P., Hirsch-Hoffmann M., Hennig, L., & Gruissem, W. (2004). Genevestigator. *Arabidopsis* microarray database and analysis toolbox. Plant Physiol. 136, 2621-2632.